EBioMedicine 50 (2019) 260–273

Contents lists available at ScienceDirect

EBioMedicine

journal homepage: www.elsevier.com/locate/ebiom

Research paper

Small molecule modulator of aggrephagy regulates neuroinflammation to curb pathogenesis of neurodegeneration

Suresh SN[a,e], Janhavi Pandurangi[b,1], Ravi Murumalla[b,1], Vidyadhara DJ[a,f,1], Lakshmi Garimella[a], Achyuth Acharya[b], Shashank Rai[a,g], Abhik Paul[c], Haorei Yarreiphang[d], Malini S Pillai[a], Mridhula Giridharan[a], James P Clement[c], Phalguni Anand Alladi[d], Taslimarif Saiyed[b], Ravi Manjithaya[a,c,*]

[a] Molecular Biology and Genetics Unit, Jawaharlal Nehru Centre for Advanced Scientific Research, Jakkur, Bangalore, India
[b] Centre for Cellular and Molecular Platforms (C-CAMP), Bangalore Life Sciences Cluster (BLiSC), Tata Institute of Fundamental Research, Bangalore, India
[c] Neuroscience Unit, Jawaharlal Nehru Centre for Advanced Scientific Research, Jakkur, Bangalore, India
[d] Department of Neurophysiology, National Institute of Mental Health and Neuro Sciences, Bangalore, India
[e] Centre for Brain Research (CBR), IISc, Bangalore, India
[f] Yale University, USA
[g] MRC Laboratory of Molecular Biology, Cambridge, UK

ARTICLE INFO

Article history:
Received 16 February 2019
Revised 13 October 2019
Accepted 20 October 2019
Available online 11 November 2019

ABSTRACT

Background: Plethora of efforts fails to yield a single drug to reverse the pathogenesis of Parkinson's disease (PD) and related α-synucleopathies.

Methods: Using chemical biology, we identified a small molecule inhibitor of c-abl kinase, PD180970 that could potentially clear the toxic protein aggregates. Genetic, molecular, cell biological and immunological assays were performed to understand the mechanism of action. In vivo preclinical disease model of PD was used to assess its neuroprotection efficacy.

Findings: In this report, we show the ability of a small molecule inhibitor of tyrosine kinases, PD180970, to induce autophagy (cell lines and mice midbrain) in an mTOR-independent manner and ameliorate the α-synuclein mediated toxicity. PD180970 also exerts anti-neuroinflammatory potential by inhibiting the release of proinflammatory cytokines such as IL-6 (interleukin-6) and MCP-1 (monocyte chemoattractant protein-1) through reduction of TLR-4 (toll like receptor-4) mediated NF-κB (nuclear factor kappa-light-chain-enhancer of activated B cells) activation. In vivo studies show that PD180970 is neuroprotective by degrading the toxic protein oligomers through induction of autophagy and subsiding the microglial activation.

Interpretation: These protective mechanisms ensure the negation of Parkinson's disease related motor impairments.

Fund: This work was supported by Wellcome Trust/DBT India Alliance Intermediate Fellowship (500159-Z-09-Z), DST-SERB grant (EMR/2015/001946), DBT (BT/INF/22/SP27679/2018) and JNCASR intramural funds to RM, and SERB, DST (SR/SO/HS/0121/2012) to PAA, and DST-SERB (SB/YS/LS-215/2013) to JPC and BIRAC funding to ETA C-CAMP.

3-MA: 3- MethylAdenine
IL-6: InterLeukin-6
LC3: Microtubule-associated protein 1A/1B-light chain 3
LPS: Lipopolysaccharide
MCP-1: Monocyte Chemoattractant Protein-1
MPTP: 1-methyl-4-phenyl-1,2,3,6-tetrahydropy
mTOR: mammalian Target Of Rapamycin
NAC: N-AcetylCysteine, ridine
NF-κB: Nuclear Factor kappa-light-chain-enhancer of activated B cells
NLRP3: NLR Family Pyrin Domain Containing 3

* Corresponding author at: Molecular Biology and Genetics Unit, Jawaharlal Nehru Centre for Advanced Scientific Research, Jakkur, Bangalore, India.
E-mail address: ravim@jncasr.ac.in (R. Manjithaya).
[1] Equal contribution.

https://doi.org/10.1016/j.ebiom.2019.10.036

PD: Parkinson's disease
Tki: Tyrosine Kinase inhibitor
TLR-4: Toll Like Receptor-4.

Research in the context

Evidence before this study

Imbalances in proteostasis are often seen in neurodegenerative diseases such as Alzheimer's and Parkinson's. This disease manifestation is aggravated by up regulation of adverse neuroinflammation reactions. However, the small molecules modulating simultaneously both processes, i.e. the neurodegenerative diseases and the neuroinflammation, are unknown.

Added value to this study

In this study, we identified and characterised a small modulator of autophagy, PD180970 exerts neuroprotection through circumventing neuroinflammation by using various model systems such as non-neuronal, neuronal and microglial cell lines as well as preclinical mouse model of Parkinson's. We showed that PD180970 clears toxic protein aggregates and curbs neuroinflammation to ameliorate the behavioural deficits.

Implications of all the available evidence

Neuroprotective ability of PD180970 is shown in preclinical neurodegenerative disease models. Thus, this study establishes PD180970 as a potential therapeutic target for neurodegenerative diseases.

1. Introduction

Parkinson's disease (PD) is the second most common neurodegenerative disease, after Alzheimer's disease; symptomatically characterized by rigidity, uncontrollable tremors, postural instability and slowness of movement [1]. A key neuropathological feature is the incidence of toxic protein clumps known as Lewy bodies in the dopaminergic (DAergic) neurons of the midbrain substantia nigra pars compacta (SNpc) [1]. The presynaptic protein α-synuclein, which is primarily involved in neurotransmitter release, forms the major constituent of Lewy bodies [2]. It has a propensity to form aggregates due to either mutations or overexpression, both in familial and sporadic Parkinson's cases, eventually perturbing the cellular proteostasis machinery [1,2]. In addition to the formation of such aggregates, cell-to-cell propagation of malformed α-synuclein in a non-cell autonomous manner leads to the spread of pathology to healthy neurons [3]. This results in the loss of over 50% of DAergic neurons in the SNpc by the time typical motor symptoms manifest in the patients [4]. The current treatment paradigm for PD revolves around supplementation of dopamine in the brain through precursors like L-DOPA or carbi-DOPA which ameliorate the symptoms, but do not curb the disease progression [4].

In PD, the continuous aggregate formation leads to an intracellular defect wherein proteostasis regulating mechanisms such as chaperones, Ubiquitin Proteasome System (UPS) and macroautophagy (henceforth autophagy) are impaired, leading to neuronal death [5]. Proof-of-principle experiments have demonstrated that clearing α-synuclein aggregates is beneficial and cytoprotective [6–8]. Toxic protein oligomers and aggregates are considered to be the substrates for autophagy machinery due to their size [9]. Genetic and pharmacological upregulation of autophagy has been shown to degrade toxic α-synuclein aggregates to exert neuroprotection in preclinical PD models [9–11].

In the symptomatic stage of PD along with massive neuronal loss, there is unregulated microglial activation leading to neuroinflammation [12]. Upon activation, microglia secrete tropic factors, cytokines, and various types of pro-inflammatory molecules such as Nitric Oxide (NO), which can upon prolonged exposure, damage and induce cell death in the surrounding neurons [13–15]. In PD, it was noted that microglial activation, accumulation of cytokines and activation of nuclear factor kappa B (NF-κB) pathway contribute to the progression of the disease [16,17]. LipoPolySaccharide (LPS) stimulated microglia have become a commonly used model to study microglial activation in vitro [16,18,19] and recent studies have shown rapid onset of neuroinflammatory responses in the SNpc as well as in the dorsal striatum on systemic injections of 1-methyl-4-phenyl-1,2,3,6-tetrahydropyridine (MPTP) in vivo [20]. The MPTP induced microglia-mediated response is triggered by the impairment of DAergic neuron function, making the MPTP-induced parkinsonian mice model suitable to study the associated neuroinflammatory changes [20]. They have also shown that MPTP mediated mitochondrial impairment activates NLRP3 inflammasome, in turn triggering proinflammatory signalling in the microglia. In the MPTP-induced mouse model of PD, the toxin's effect on activation of microglia is observed allowing it to serve as model for neuroinflammation mediated neurodegenerative cascades[14] . Upon MPTP and/or LPS assault, a cascade of enzymes and transcription factors are activated, resulting in the release of numerous pro-inflammatory molecules such as NO, TNF-α (Tumor Necrosis Factor α), IL-1β (Interleukin 1β) and IL-6 (Interleukin 6), which create an inflammatory micro-environment and can result in neuronal cell death [14]. Thus, anti-inflammatory drugs and strategies to restrict the aberrant microglial activation to attenuate neurodegeneration can prove to be a valuable therapeutic strategy.

During the progression of PD, neuronal death owing to toxic protein aggregates invokes an adverse neuroinflammatory response which further propagates neuronal loss, thus creating a vicious cycle. This multifactorial nature of PD pathogenesis and progression is hindering the clinical success of drugs that independently target either autophagy or inflammation, leaving patients dependent on symptomatic relief.

Towards this, we hypothesised that modulating both neuronal autophagy and neuroinflammation simultaneously could exert neuroprotection *in toto*. One of the approaches of alleviating the neurodegeneration disease phenotypes involves suppression of proteins that are elevated in patients suffering from PD related neurodegeneration. Tyrosine kinase levels were found to be elevated in such patient brains and downregulation of their expression have been correlated with a decrease in levels of pathological protein aggregates [21]. In this line, we inhibited the C-Abelson (c-Abl) tyrosine kinase and investigated its effectiveness of exerting neuroprotection. Inhibition of this kinase activity has been suggested as a potential target in the treatment of PD [22,23]. PD180970 is a potent ATP competitive Bcr-Abl inhibitor (TKi) for c-Abl kinase at nanomolar concentration [24]. While the effect of this molecule on cancer progression has been well addressed [25], its neuroprotective potential is unclear.

In this study, we demonstrate that the small molecule PD180970 exerts neuroprotection by simultaneously regulating the proteostasis machinery and neuroinflammation. PD180970 abrogates α-synuclein mediated toxicity in mammalian cells through autophagy induction in a mammalian target of rapamycin (mTOR) independent manner. Interestingly, in vitro studies in microglial and neuron-microglial cell co-cultures have also demonstrated reduction of neuroinflammation as well as modulation of cytokine release on PD180970 treatment. We also noted that PD180970 protects dopaminergic neurons in a preclinical mouse model of PD by inducing autophagy and aggregate clearance. In addition, PD180970 also inhibited microglial activation and proliferation. This two-

pronged strategy led to the amelioration of motor behavioural deficits. Thus, PD180970 through its poly-pharmacological actions by simultaneously clearing α-synuclein aggregates and attenuating neuroinflammation provides a potential disease-modifying treatment strategy for PD.

2. Materials and methods

2.1. Cell culture

HeLa cells were cultured in DMEM medium with 10% FBS. Cells were maintained at 37 °C in presence of 5% CO_2. The immortalized rat mesencephalic dopaminergic cells (N27cells) and Rat microglial cells (BV2 cells) were obtained from Dr. Anumantha Kanthasamy (Iowa State University) as a gift [26]. Cells were grown in RPMI 1640 medium containing 10% Fetal Bovine Serum (FBS), 2 mM L-glutamine, 50 U Penicillin and 50 μg/ml Streptomycin.

2.2. Reagents

Lipopolysaccharide O111:B4 (L4391), MPP^+ (D048) , MPTP (1-methyl-4-phenyl-1, 2, 3, 6-tetrahydropyridine, M0896), H_2O_2 (H1009), PD180970 (PZ0142), anti LC3 antibody (L7543), 3-MA (M9281), Penicillin and Streptomycin (P4333), DMEM (D5648), DMEM F-12 (D8900), DAB (3, 3′-Diaminobenzidine, D3939), Cy3 conjugated anti-rabbit secondary antibody (C2306), FITC conjugated anti-rabbit secondary antibody (F7512) and Trypsin EDTA (59418C) were purchased from Sigma-Aldrich. Pam3CSK4, PolyI:C and HEK-Blue Detection media were obtained from InvivoGen (San Diego, CA). Antibodies such as anti-phospho P70S6K T389 antibody (9239) and total P70S6K antibody (9202), anti-phospho 4E-BP1T37/46 antibody (2855) and total 4E-BP1 antibody (9452) and anti-rabbit IgG HRP (7074) were purchased from Cell Signaling Technology. Cell Titre Glo® kit (G 7571) was from Promega. Anti-β-tubulin (MA5-16,308) antibody was from Thermo Scientific. Anti-mouse IgG, and HRP (172–1011) antibody was from Bio-Rad. Anti-ubiquitin antibody (NB300-130) was purchased Novus Biologicals. Anti-p62 antibody (PM045) was purchased from MBL International. Anti-Tyrosine Hydroxylase (N196) and anti-A11 (AB9234) antibodies were from Santa Cruz Biotechnology and Merck Millipore respectively. Bafilomycin A1 (11,038) was from Cayman chemical. Vectastain Elite ABC Kit (PK-6101) was procured from VECTOR laboratories.

For autophagy related assays, the plasmids such as ptf LC3 [27] (gift from Tamotsu Yoshimori, Addgene # 21,074), EGFP-α-synuclein [28] (gift from David Rubinzstein, Addgene number # 40,822) are used.

2.3. Immunoblotting

Samples were electrophoresed using SDS-PAGE (8–15%) and then transferred onto PVDF membrane. The blots were stained with Ponceau S to ensure the proper transfer of proteins. Then, the blots were probed with appropriate primary antibodies for overnight followed by incubation with HRP-conjugated secondary antibody. Signals from blots were developed using enhanced chemiluminescence substrate (Clarity, Bio-Rad). Imaging was done using a gel documentation system (G-Box, Syngene, UK). Using ImageJ software, band intensities were quantified.

2.4. Neuronal cell viability assay

SH-SY5Y (human neuroblastoma) cells were seeded onto 96 well plate and transfected with EGFP-α-synuclein plasmid and allowed to express for 48 h. Then, they were treated with PD and/or 3-MA for 24 h and its viability was measured using CellTitre-Glo® assay.

3. Autophagic assays

3.1. Western based autophagic assays

At sub-confluency level, equal number of HeLa cells were seeded in a 6-well plate and allowed it to attach. Then, the cells were treated with appropriate small molecules such as PD180970 (1 μM) and baf A_1 (100 nM) for 2 h and cell lysates were prepared. Immunoblotting was performed for probing the autophagic related proteins such as LC3, phospho and total P70S6K, 4EBP1. Conversion of LC3-I to lipidated LC3-II form would indicate the enhancement of autophagy.

3.2. Microscopy based autophagic assay

Cells were seeded onto 60 mm dishes and allowed to attach. Then, the cells were transfected with mRFP-EGFP-LC3 plasmid construct and allowed to express for about 48 h. Following that, the cells were trypsinised and seeded onto either 12 or 24 well plates containing coverslips and allowed to attach. It was then treated with the small molecule for 2 h and coverslips were processed for imaging. In this standard assay, the autophagosomes would appear as yellow whereas autolysosomes would be red as EGFP gets quenched at lysosomal acidic pH6.

4. Aggregate clearance assay

Equal number of SH-SY5Y cells were seeded onto 6-well plates and allowed to attach overnight. Then, EGFP-α-synuclein was transiently transfected for 48 h. After that, the cells were treated with PD180970 or 3-MA or both for 24 h. Tthe lysates were prepared and immunoblotting was performed.

5. Treatment paradigm for neuroinflammation assays

Cells at 60–70% confluency were harvested and seeded in 96 well plates at a seeding density of 8×10^3 cells/ well.

5.1. Oxidative stress model (Hydrogen peroxide)

Cells were co-treated with 75 μM H_2O_2 in the presence and absence of compounds for 8 h. Treatments were made in complete RPMI medium containing 2% FBS. Cell survival was measured using MTS assay which was performed according to the protocol given by the manufacturer.

5.2. Neuroinflammation model (LPS)

Cells were co-treated with 1 μg/ml LPS in the presence and absence of compounds for 48 h. Treatments were made in complete RPMI medium containing 10% FBS. The concentration of Nitric oxide released was measured using the Griess Assay (Sigma) according to the manufacturer's protocol.

5.3. HEK-Blue™ TLR2/4 assay

Hek-Blue™ TLR-2 and TLR-4 Cells were obtained from Invivogen Culture treatment and assay was performed as per the manufacturers recommended protocol.

5.4. Media transfer assay

BV2 cells were cultured in 96-well plates at seeding density of 1×10^4 cells/well and treated with LPS 1 g/ml in the presence and absence of compounds for 48 h. The media was then transferred to N27 cells cultured in 96-well plates at seeded of 8×10^3 cells/well

for 24 h. N27 cell survival was then measured using MTS assay which was performed according to the protocol given by the manufacturer.

5.5. Neuron- microglia co-culture

N27 and BV2 cells were co-cultured in Corning HTS Transwell Plates, N27 in the lower well of the 24 well plates and BV2 in the 0.4 μm porous permeable support inserted on top of the 24 well. BV2 cells were treated with LPS 1 μg/ml in the presence and absence of 1 μM of PD for 30 h. The survival of N27 cells was then measured using MTS Assay. Media was collected from all conditions and tested for concentration of Nitric oxide using the Griess Assay as well as for cytokine profile using Luminex multiplexing assay.

6. Animal studies

JNCASR Institute Animal Ethical Committee (IAEC) approved the animal experiments and they were conducted as per the guidelines of the Committee for the Purpose of Control and Supervision of Experiments on Animals (CPCSEA). Male C57BL/6J mice (3 to 4 months old) were used for experiments. Animals were maintained at JNCASR animal house facility.

7. MPTP toxicity model

The acute MPTP model has profound neuronal loss i.e., around 50% loss of dopaminergic neurons in seven days that is considerably higher than subchronic model [29]. Three to four months old male mice were randomly allotted to three-study cohort namely control ($N=6$), MPTP ($N=5$) and MPTP+Co ($N=6$). The MPTP group animals received intraperitonial injections of MPTP.HCl (23.4 mg/kg of body weight) 4 times at 2 h interval, whereas the control group received only saline. The MPTP+Co regimen involved administration of MPTP along with small molecule PD180970 (5 mg/kg of body weight). In this regimen, PD was administered daily at the same dosage for 7 days since the first injection. Following the treatment, the animals were sacrificed, and the brains were processed for immunohistochemistry.

8. Immunohistochemistry

The mice were anaesthetized using halothane BP (Piramal Healthcare, India) inhalation and perfused transcardially with normal saline followed by 4% paraformaldehyde (PFA) in 0.1 M phosphate buffer, pH 7.4. The brains were removed quickly and post-fixed with 4% PFA for 24–48 h at 4 °C. Following cryoprotection in 15 and 30% sucrose (HiMedia, MB025), 40-µm-thick coronal cryosections of midbrain were collected serially on gelatinized slides.

Immunoperoxidase labelling was performed as described earlier [30]. Endogenous peroxidase was quenched by incubating the sections with H_2O_2 (0.1%) followed by blocking with BSA (3%) for 4 h at room temperature. Thereafter, the sections were incubated with primary TH antibody (1:500) followed by biotin conjugated secondary antibody (1:200). Avidin-biotin complex solution (1:100) was used for tertiary labelling. Staining was developed using 3′−3′-diaminobenzidine (0.05%) chromogen in acetate imidazole buffer (pH 7.4 and 0.1 M).

A sequential staining protocol was followed for immunofluorescent labelling on adjacent sections. The sections were stained for TH/LC3, TH/A11 and Iba1 antibodies followed by image acquisition in DeltaVision Elite widefield microscope.

9. Densitometry based TH$^+$ intensity quantification

High magnification images of TH stained nigral dopaminergic neurons were acquired for the offline quantification of TH expression. Image analysis system (Q Win V3, Leica) was used to measure the intensity. Around 200 dopaminergic neurons per animal were assessed on a scale of 0–255 (gray scale) where 0 suggests intense staining and 255 suggests absence of staining. The results were derived from cumulative mean for each sample and quantitated. Note that the lower grey values indicate the higher protein expression and vice versa.

10. Behavioural studies

C57BL/6J mice strain of 3 to 4 months old, male animals were used for behavioural study. Experiment performers were blinded to the drug injected animals. Experimenters handled animals for 3 consecutive days prior to the appropriated behaviour training. Rotarod and open field tests were performed on the same animal cohorts. The paradigm was strategized and conducted in an order of low to high stress activity per day. So, the open field and rotarod was conducted in forenoon and afternoon respectively. Mice were habituated for 15 min prior to the commencement of behaviour paradigm and also weighed to ensure their good health. The light intensity of 100 lx was maintained during training and experimental period. Mice were grouped into three cohorts namely, control, MPTP and MPTP+Co.

11. Rotarod

The custom-made rotatod instrument made at National Centre for Biological Sciences (NCBS) was used to perform rotarod paradigm and details about the instrument have been described earlier [6]. Animals were trained for 5 consecutive days prior to drug treatments. The rpm for days 1, 2, 3 were 5–10, 11–15 and 16–20 respectively, and 20 rpm for fourth and fifth training day. Mice were trained 3 times with 5 min intervals between each trial. During the actual experiment, the rotarod was started at 20 rpm for 60 s and their latency to fall was calculated. After each trial, the equipment was wiped with 70% ethanol and allowed to dry before the start of next trial. All trials were recorded using DSLR camera (Nikon D5100) and the latency to fall was noted manually.

12. Open field test

The open field arena was custom-made at JNCASR and its details were previously reported [6]. Animals were habituated in the arena for 2 consecutive days before the actual trial. The animals were allowed to explore the centre and peripheral zones of the open field arena for 5 min and video (SONY® colour video camera, SSC-G118, India) was recorded using software (SMART v3.0.04, Panlab, Harvard Apparatus, USA). The arena was wiped with 70% ethanol and allowed to dry at the end of each trial. The distance travelled by the animals was analyzed and plotted for all cohorts.

13. Number of TH-ir dopaminergic neurons and Iba1-ir microglia in SNpc

Quantification of the absolute number of TH-ir dopaminergic neurons was performed using unbiased stereology [31,32] using a 10X objective of Olympus BX61 Microscope equipped with StereoInvestigator (Software Version 8.1, Micro-brightfield Inc., Colchester, USA). Stereological quatification for dopaminergic neuronal number was performed using optical fractionator probe of the StereoInvestigator [6,7]. The TH-ir cells were counted using high magnification oil immersion objective (100X), with a regular

grid interval of 22,500 μm^2 ($x = 150\,\mu m$, $y = 150\,\mu m$) and counting frame of size 3600 μm^2 ($x = 60\,\mu m$, $y = 60\,\mu m$). The mounted section thickness approximated between 24 and 25 µm. We applied guard zone of 4 μm on either side, thus providing 16–17 µm of z-dimension to the optical dissector. We began the quantification at the first anterior appearance of SNpc to the caudal most part in both hemispheres and added to derive total numbers. We measured the volume of SNpc on principles of contour planimetry by delineating the nigra with 10X objective of Olympus BX61 Microscope (Olympus Microscopes, Japan) during stereological quantification.

For counting microglial cells, immunofluorescently labelled images of SNpc Iba1-ir cells were captured using DeltaVision microscope (GE Healthcare, USA) using 4 X objectives, at laser excitation of 488 nm for FITC. Images were processed using SoftWorx (GE Healthcare, USA) and the number of Iba1-ir microglial cells per microscopic field were counted using ImageJ (1.48v program, NIH, USA). A cumulative mean was derived for the numbers after sampling microglial cells from eight microscopic fields per animal. Values were expressed as percentage change in numbers with respect to control (or number of cells per microscopic field) [33].

14. Statistical analyses

Statistical tests used in this study are unpaired Student's *t*-test and ANOVA (one-way or two-way) followed by post-hoc Bonferroni test using Prism 6.0 Software (GraphPad, San Diego, CA). Error bars indicate mean ± SEM.

15. Results

15.1. PD180970 induces autophagy in mammalian cells and mouse midbrain

To investigate if PD180970 regulates autophagic flux in mammalian cells, we performed a fluorescence microscopy-based tandem RFP-GFP-LC3 assay and immunoblotting experiments. PD180970 (1 μM) treatment enhanced the autophagic flux as revealed by the significant increase in both autophagosomes (~4 fold, $P < 0.001$, compared to control; Fig. 1A) and autolysosomes (~2 fold, $P < 0.001$, compared to control; Fig. 1a). Apart from the increased autophagy flux, the increase in autophagosome numbers suggested that PD180970, in addition, might enhance autophagosome biogenesis and/or maturation.

LC3 immunoblotting revealed that PD180970 ($P < 0.001$, versus untreated, Fig. 1b) treatment enhanced the conversion of LC3-I to LC3-II as compared to untreated. Treatment with lysomotrophic agents such as bafilomycin A_1, displayed more LC3-II accumulation in the presence of PD180970 when compared to only bafilomycin A_1 ($P < 0.001$, versus untreated, Fig. 1b), indicating that PD180970 is an autophagy inducer.

In DAergic neurons of SNpc in mouse midbrain, upon PD180970 treatment, the number of LC3 positive puncta was significantly enhanced than that of vehicle ($P < 0.001$, Vehicle versus PD180970, Fig. 5a), suggesting the induction of autophagy. Thus, these results indicate that PD180970 induces autophagy in mammalian cells as well as DAergic neurons of SNpc in mouse midbrain.

15.2. PD180970 is an mTOR-independent autophagy inducer

We next investigated if the modulation of autophagy by PD180970 is via mTOR-dependent or independent mechanisms. The phosphorylation status of mTOR substrates such as P70S6K (Ribosomal protein S6 kinase beta-1) and 4EBP1 (eIF4E-binding protein 1) reveals mTOR activity, as the phospho-forms of these substrates are present when mTOR is active [34]. The phosphorylated P70S6K levels and isoforms of 4EBP1 in PD180970 treatments are comparable to that of nutrient-rich conditions suggesting that PD180970 acts via an mTOR-independent pathway (Fig. 2a).

15.3. PD180970 exerts cytoprotection against α-synuclein toxicity that is autophagy-dependent

Next, we examined an aggregate clearance and neuroprotection potential of PD180970 using immublotting and cell viability assays.

To assess the potential of toxic protein clearance by PD180970, we performed an aggregate clearance assay. Upon PD180970 treatment for 48 h, the level of α-synuclein was significantly reduced than untreated ($P < 0.01$, versus untreated, Fig. 2b). In co-treatment group of 3-methyl adenine (the autophagy inhibitor) and PD180970, the level of α-synuclein was comparable to that of untreated ($P > 0.05$, versus 3-MA, Fig. 2b). Also, the α-synuclein protein level was significantly more than PD180970 only assay ($P < 0.001$, versus untreated, Fig. 2b). These indicated that PD180970 has an ability to clear α-synuclein protein in an autophagy-dependent manner.

Interestingly, in the presence of α-synuclein, ubiquitin ($P < 0.01$, versus untreated, Fig. S5 a and b) as well as p62 ($P < 0.01$, versus untreated, Fig. S5 c and d) levels increased significantly with concomitant increase in presence of toxic oligomers ($P < 0.01$, versus untreated, Fig. S6) as compared to untreated cells. These results indicated that α-synuclein elevated ubiquitinated protein adducts inside cells. As expected, upon treatment of PD180970 to α-synuclein expressing cells, the ubiquitin ($P < 0.01$, versus untreated, Fig. S5 a and b), p62 ($P < 0.05$, versus LPS, Fig. S5 c and d) and toxic oligomer levels ($P < 0.01$, versus untreated, Fig. S6) gets reduced significantly than untreated ones.

We examined the cytoprotective ability of PD180970 in an α-synuclein toxicity model of human neuroblastoma SH-SY5Y cells. When α-synuclein is overexpressed, cell viability is significantly compromised as compared to vector control or untransfected cells. Cell viability of α-synuclein over-expressing cells was significantly enhanced when treated with PD180970 ($P < 0.001$, versus untreated, Fig. 2b) compared to untreated cells. Interestingly, this apparent cytoprotection is significantly reduced when cells treated with PD180970 ($P < 0.05$, versus 3-MA, Fig. 2b) are co-administered with the pharmacological autophagy inhibitor, 3-Methly adenine (3-MA). There is no significant decrease in viability of α-synuclein overexpressing cells when only treated with 3-MA, ruling out the possibility of its toxicity ($P > 0.05$, versus 3-MA, Fig. 2b). Thus, PD180970 exerts its cytoprotective effects in an autophagy-dependent manner.

These results indicated that PD180970 exert the ability to clear toxic α-synuclein protein aggregates in an autophagy-dependent manner.

15.4. PD180970 protects dopaminergic neurons from LPS-induced death in vitro

Neuroinflammation is one of the crucial pathological factors that propel the pathogenesis of Parkinson's disease [14]. We asked whether PD180970 possesses anti-neuroinflammatory potential. Towards this, microglial (BV2) cells were treated with LPS (1 $\mu g/ml$) in the presence or absence of PD180970 (0.1 nM to 10 μM) and conditioned media was tested for nitrite release. Upon LPS addition, the nitrite release was significantly higher than untreated cells, indicating an inflammatory response ($P < 0.01$, versus control, Fig. 3d). We observed a significant reduction in nitrite release upon addition of PD180970 to activated microglia in a dose-dependent manner ($P < 0.05$, versus LPS, Fig. 3d) indicating its anti-inflammatory effect. In this scenario, we noted the sig-

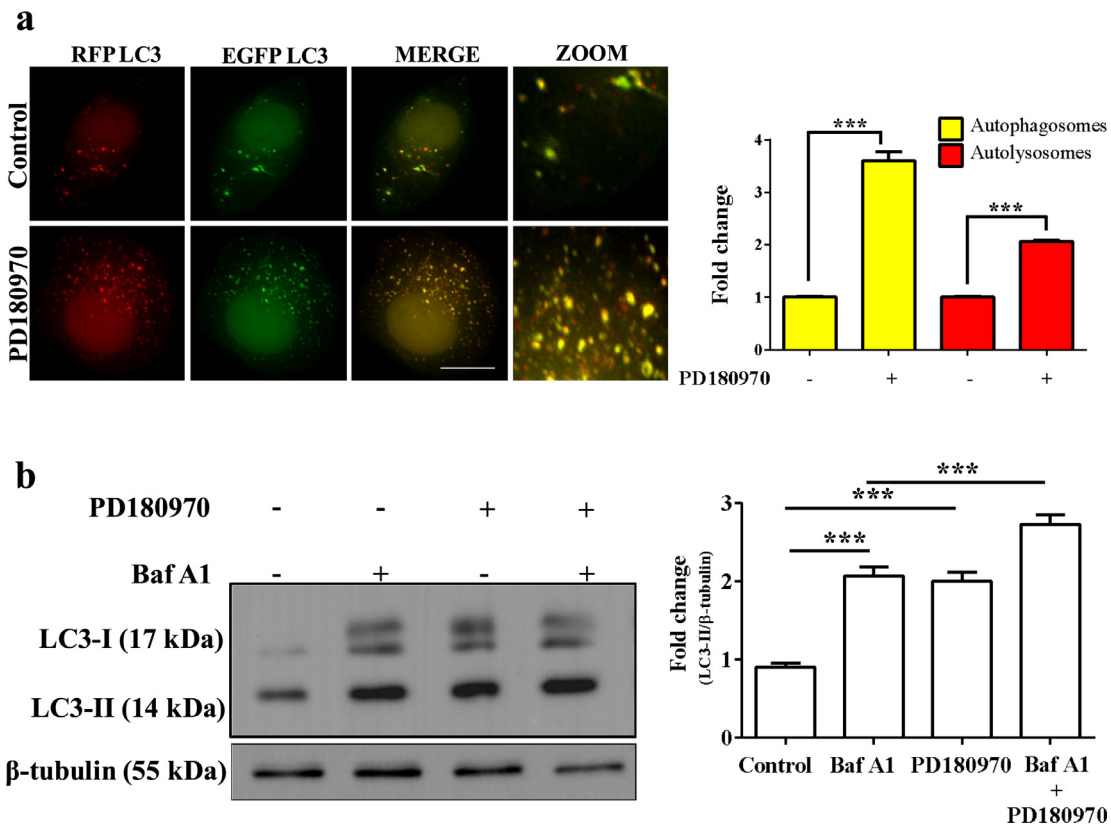

Fig. 1. PD180970 was an inducer of autophagy. (a) Microscopy images of HeLa cells in tandem RFP-EGFP-LC3 assay treated with PD180970 for 2 h duration in growth medium. Autophagosomes appeared as yellow puncta whereas autolysosomes appeared as red puncta. Upon PD180970 treatment, the fold change in autophagosomes and autolysosomes were quantified (n= at least 50 cells and three independent experiments). Scale bar was 15 μm. Statistical analysis was performed using Student's t-test. Error bars, mean ± SEM. ***-$P < 0.001$. (b) Western blot for LC3 processing assay in HeLa cells treated with PD180970 (2 h) with or without bafilomycin A_1 in growth medium. Normalized LC3-II protein levels of various treatments were quantified ($n = 3$ and three independent experiments). β-tubulin served as a loading control. Statistical analysis was performed using one-way ANOVA and post-hoc Bonferroni test. Error bars, mean ± SEM. ***-$P < 0.001$.

nificant enhancement in viability of N27 cells (Fig. 3a). To validate this, we evaluated the anti-neuroinflammatory mediated neuroprotective effect of PD180970 by co-culturing the neurons with microglia that were activated by LPS. LPS treated BV2 cells caused ~50% cell death in N27 cells with concomitant increase in nitrite release indicating the neuroinflammation mediated cell death (~5 fold, $P < 0.05$ versus untreated, Fig. 3b). Upon PD180970 (1 μM) addition to activated microglia, we observed a significant increase in viability of DAergic neurons (~50%, $P < 0.05$ versus LPS, Fig. 3e) and reduction of nitrite release (~50%, $P < 0.05$ versus LPS, Fig. 3b). These results indicate that PD180970 protects DAergic neurons against LPS-induced cell death.

We further tested the ability of PD180970 to prevent the H_2O_2 (hydrogen peroxide) mediated death of DAergic neurons. Towards this, N27 DAergic cells were treated with hydrogen peroxide (75 μM) in the presence and absence of PD180970 (H_2O_2, 10 nM to 10 μM) for 8 h. PD180970 was observed to have no significant neuroprotective effect on H_2O_2 mediated oxidative stress-induced toxicity in N27 cells (Fig. S1). These results clearly indicate the in vitro anti-neuroinflammatory mediated neuroprotective effect of PD180970.

15.5. PD180970 ablates LPS-induced release of IL-6 and MCP-1

In the central nervous system, chemokines such as MCP-1 and IL-6 are needed to recruit the immune-related cells at the sites of inflammation [35]. LPS treated microglial cells displayed considerable increase in the levels of IL-6 (~17 fold, $P < 0.001$ versus untreated, Fig. 4a) and MCP-1 (~10 fold, $P < 0.01$ versus untreated, Fig. 4b) secretion. Upon PD180970 treatment, we observed a significant reduction in the level of both IL-6 (~73%, $P < 0.001$ versus LPS, Fig. 4a) and MCP1 (~84%, $P < 0.01$ versus LPS, Fig. 4b) released by LPS-induced microglial cells compared to that of untreated. These data show the ability of PD180970 to decrease the release of proinflammatory cytokines such as MCP-1 and IL-6.

15.6. PD180970 lowers LPS-induced NF-κB activity that is mediated by TLR2 and TLR4

Mechanism of PD180970 action was deduced through treating HEK-Blue™ TLR4, HEK-Blue™ TLR3 and HEK-Blue™ TLR2 cells with LPS (10 ng/ml), PolyI:C (1 μg/ml) and Pam3CSK4 (10 ng/ml) respectively, for 16 h in the presence or absence of the PD180970 (1 nM to 100 μM). Quantification of NF-κB induced SEAP (full form) release indicated that the compound had a significant inhibitory effect on SEAP release in HEK-Blue™ TLR4 and HEK-Blue™ TLR2 cells, but not in HEK-Blue™ TLR3 cells, suggesting that its mechanism of action is via the NF-κB downstream signalling pathway. Fig. 4 shows the effect of a 16 h co-treatment of PD180970 with LPS 10 ng/ml on HEK-Blue™ TLR4 cells.

15.7. PD180970 mitigates MPTP-induced neuronal loss

In order to test if the autophagy-dependent cytoprotection of PD180970 (5 mg/kg body weight) extends in an in vivo situation, we employed a preclinical mouse model of PD i.e. MPTP toxicity model (Fig. S2) [29]. Mice were randomly divided into Control, MPTP and MPTP+Co groups. Seven days post-treatment, they

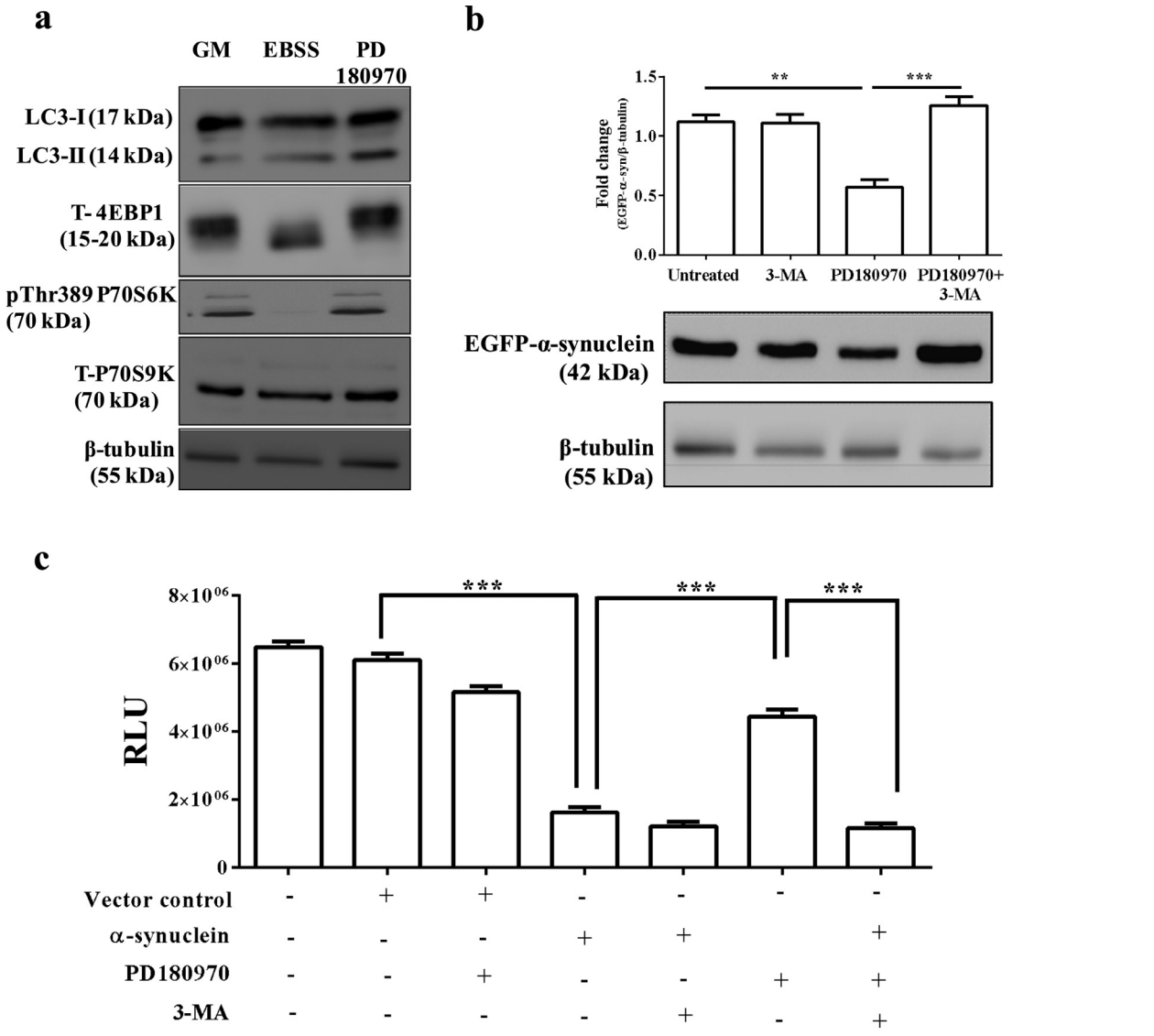

Fig. 2. PD180970 cytoprotected neuronal cells against EGFP-α-synuclein toxicity in an mTOR-independent manner. (a) Western blots indicating the protein levels of mTOR substrates -P70S6K (phospho and total form) and 4EBP1 (phospho and total form) upon various treatments such as growth medium (GM), EBSS (starvation medium) and PD180970. β-tubulin served as a loading control. (b) Western blot images of EGFP-α-synuclein protein levels in various treatment groups such as untreated, PD180970 only, 3-MA only and PD180970 and 3-MA together and quantitated their levels that are normalized with β-tubulin. (c) Plot represents the cell viability of SH-SY5Y that overexpresses EGFP-α-synuclein treated with PD180970 in presence or absence of 3-MA (the pharmacological inhibitor of autophagy). This cell viability assay was performed using CellTitre Glo® (Promega) kit. Higher RLU (relative light units) means presence of more number of viable cells and vice-versa (Three independent experiments). Statistical analysis was performed using one-way ANOVA and post-hoc Bonferroni test. Error bars, mean ± SEM. ***-$P < 0.001$.

were sacrificed, and brain sections were immobilized onto slides (Fig. S2). Upon MPTP administration, around 70% DAergic neurons were ablated in the SNpc region of brain with a concomitant reduction in the striatal dopamine levels [29]. In MPTP+Co regimen, MPTP was administered along with PD180970 on the same day. Tyrosine hydroxylase (TH), a dopaminergic neuronal marker was used to quantify neuronal numbers using unbiased stereology while the cellular TH expression was measured by densitometry. MPTP administration, resulted in a significant loss of DAergic neurons and reduced TH expression vis-á-vis the saline cohort ($P < 0.001$, versus saline, Fig. 5e and f) confirming the MPTP-induced neuronal loss [29]. Interestingly, the neuronal number in MPTP+Co cohort was unaffected and was significantly more than that of MPTP exposed cohort, indicating the neuroprotective potential of PD180970 ($P < 0.001$, MPTP versus MPTP+Co, Fig. 5e and f). The TH expression in MPTP+Co cohort animals was significantly better retained than the MPTP treated cohort ($P < 0.01$, MPTP versus MPTP+Co, Fig. S4). The reduction in SNpc volume due to MPTP administration was significantly alleviated upon PD180970 administration ($P < 0.05$, MPTP versus MPTP+Co, Fig. S4). These results demonstrate the neuroprotective ability of PD180970 in a preclinical mouse model of PD.

15.8. PD180970 clears toxic protein oligomers by inducing autophagy in SNpc

We next examined the ability of PD180970 to induce autophagy to clear toxic protein oligomers in SNpc. The intracellular accumulation of misfolded protein oligomers exerts cellular toxicity by promoting the sequestration of vital cellular components [36]. In MPTP-treated cohort, there was significant down-regulation of LC3B puncta per neuron ($P < 0.05$, vehicle versus MPTP, Fig. 5a and b) along with upregulation of toxic protein oligomers, than that of saline-treated ($P < 0.001$, vehicle versus MPTP, Fig. 5c and d). This observation is in line with the previous studies using this mouse model to study neurodegeneration [6,36]. Thus, autophagy is per-

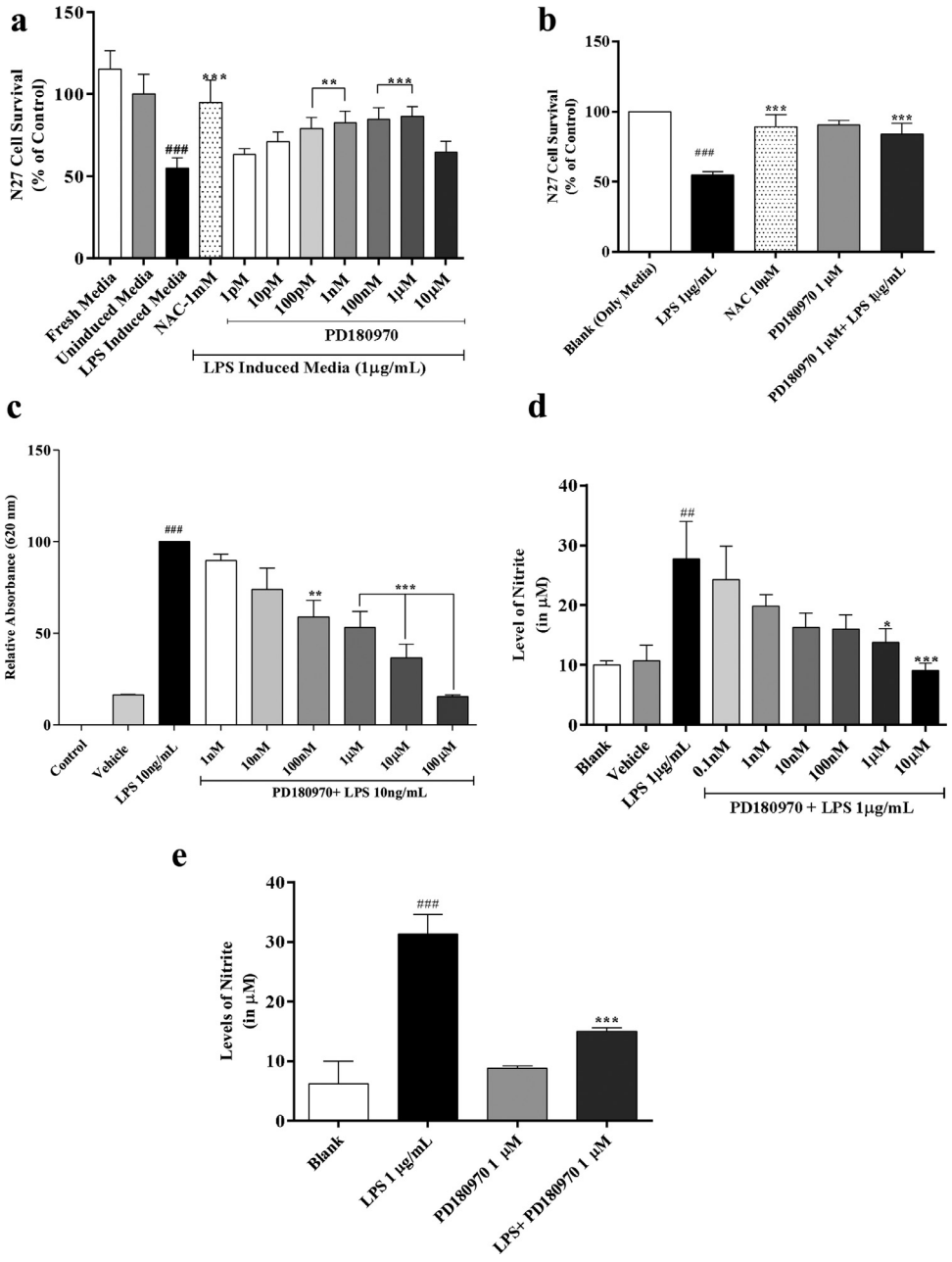

Fig. 3. PD180970 exerted anti-neuroinflammatory potential revealed through neuron-glia co-culture. (a) Induced media from BV2 cells containing 1 μg/ml LPS and varying concentrations of PD180970 from 0–10 μM were collected after 48 h of culture and then added to N27 cells. N27 cell survival was measured by MTS assay after 24 h of incubation of cells in the induced media. Data represents the group mean ± SEM; $n = 4$ per condition and experiments were repeated three times. ### ($P < 0.001$) indicates significant difference compared to blank control cells. * ($P < 0.05$); *** ($P < 0.001$); indicates significant difference compared to LPS treated cells. (b) N27-BV2 co-culture were treated with PD180970 at a concentration of 1 μM in the presence and absence of LPS 1 μg/ml and assayed for N27 cell survival at 30 h. MTS assay was performed to determine the percentage N27 survival. LPS (1 μg/ml) was used as control for nitrite release. NAC was used as positive control for anti-inflammatory effect. Co-treatment of PD180970 with LPS caused significant decrease in nitrite level as compared to LPS alone. Data represents the group mean ± SEM; $n = 4$ per condition and experiments were repeated three times. ### ($P < 0.001$) indicates significant difference compared to blank control cells. *** ($P < 0.001$) indicates significant difference compared to LPS treated cells. (c) HEK-Blue™ TLR4 cells were treated with PD180970 at a concentration range of 1nM-100 μM in the presence of LPS 10 ng/ml and assayed for SEAP activity for 12 h. SEAP activity was quantified using HEK-Blue™ Detection. LPS (10 ng/ml) was used as control for SEAP activity. PD180970 co-treated with LPS 10 ng/ml caused significant reduction in levels of NF-κB induced SEAP as compared to LPS alone. Data represents the group mean ± SEM; $n = 4$ per condition and experiments were repeated three times. ### ($P < 0.001$) indicates significant difference compared to control cells. ** ($P < 0.01$); *** ($P < 0.001$) indicates significant difference compared to LPS treated cells. (d) BV2 cells were treated with PD180970 at a concentration range of 0.1 nM- 10 μM in the presence of LPS 1 μg/ml and assayed for concentration of nitrite released for 48 h. Griess assay was performed to determine the concentration of nitrite released. LPS (1 μg/ml) was used as control for nitrite release. PD180970 caused significant reduction in levels of nitrite as compared to LPS alone. Data represents the group mean ± SEM; $n = 4$ per condition and experiments were repeated three times. ## ($P < 0.01$) indicates significant difference compared to blank control cells. * ($P < 0.05$); *** ($P < 0.001$) indicates significant difference compared to LPS treated cells. (E) N27-BV2 co-culture was treated with PD180970 at a concentration of 1 μM in the presence and absence of LPS 1 μg/ml and assayed for Nitrite release at 30 h. Griess assay was performed to determine the concentration of Nitrite released by BV2. LPS (1 μg/ml) was used as a microglial activator. Co-treatment of PD180970 with LPS caused a significant decrease in nitrite release as compared to LPS alone. Data represents the group mean ± SEM; $n = 4$ per condition and experiments were repeated three times. ### ($P < 0.001$) indicates significant difference compared to blank control cells. *** ($P < 0.001$) indicates significant difference compared to LPS treated cells.

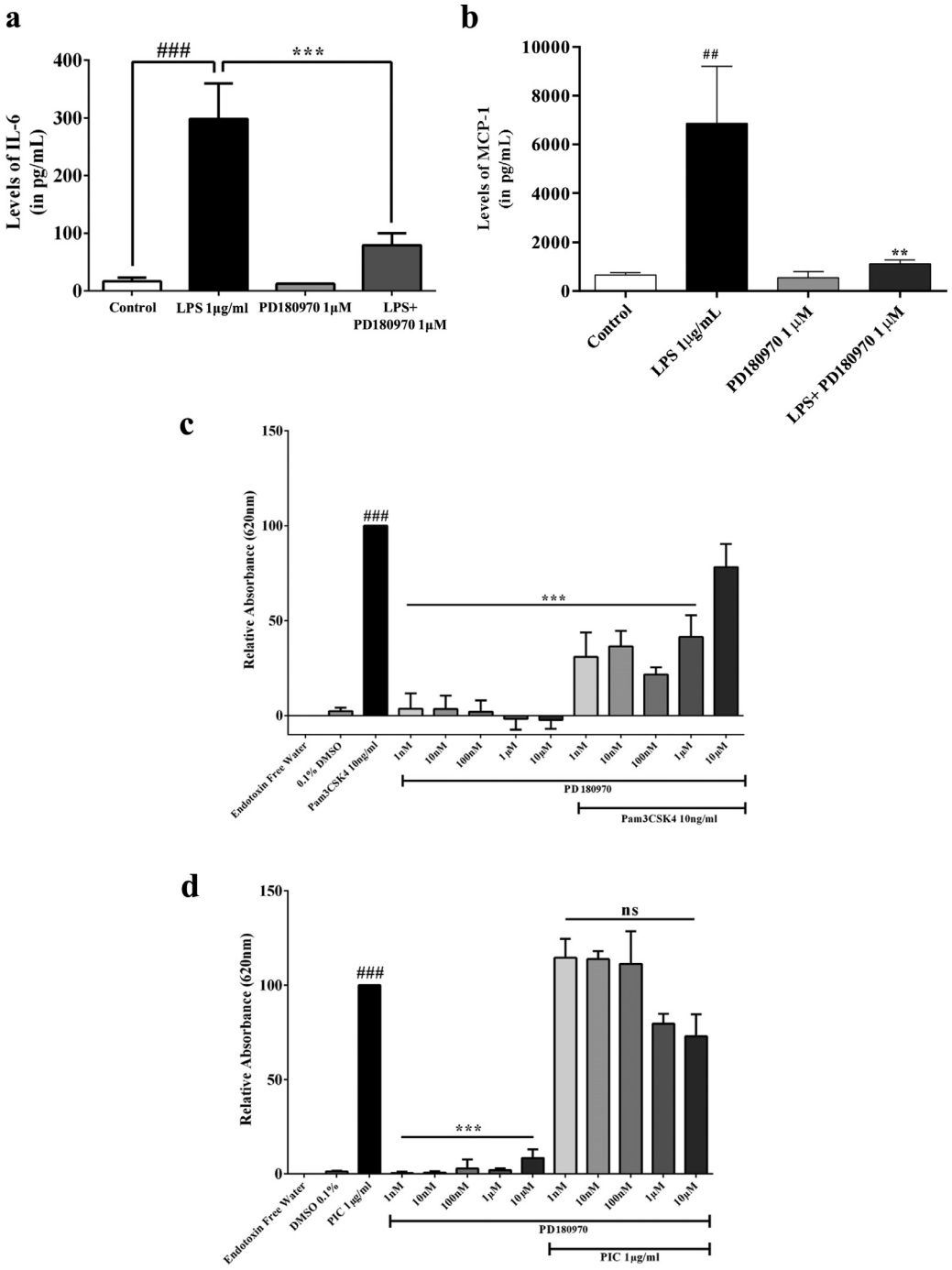

Fig. 4. PD180970 ablated release of pro-inflammatory cytokines such as IL-6 and MCP-1. (a) N27-BV2 co-culture was treated with PD180970 at a concentration of 1 μM in the presence and absence of LPS 1 μg/ml and assayed for Nitrite release at 30 h. Luminex multiplexing assay was performed to determine the concentration of IL-6 released. LPS (1 μg/ml) was used as control for IL-6 release. PD180970 caused significant reduction in levels of IL-6 as compared to LPS alone. Data represents the group mean ± SEM; $n = 4$ per condition and experiments were repeated twice. $^{###}$ ($P < 0.001$) indicates significant difference compared to blank control cells. *** ($P < 0.001$); indicates significant difference compared to LPS treated cells. (b) N27-BV2 co-culture was treated with PD180970 at a concentration of 1 μM in the presence and absence of LPS 1 μg/ml and assayed for Nitrite release at 30 h. Luminex multiplexing assay was performed to determine the concentration of MCP-1 released. LPS (1 μg/ml) was used as control for MCP-1 release. PD180970 caused significant reduction in levels of MCP-1 as compared to LPS alone. Data represents the group mean ± SEM; $n = 4$ per condition and experiments were repeated twice. $^{#}$ ($P < 0.05$) indicates significant difference compared to blank control cells. ** ($P < 0.01$); indicates significant difference compared to LPS treated cells. (c) HEK-Blue TM TLR2 cells were treated with PD180970 at a concentration range of 1 nM-10 μM in the presence of Pam3CSK4 10 ng/ml and assayed for SEAP activity for 16 h. SEAP activity was quantified using HEK-Blue^{TM} Detection. Pam3CSK4 (10 ng/ml) was used as control for SEAP activity. PD180970 co-treated with Pam3CSK4 10 ng/ml caused significant reduction in levels of NF-κB induced SEAP as compared to Pam3CSK4 alone. Data represents the group mean ± SEM; $n = 4$ per condition and experiments were repeated three times. $^{###}$ ($P < 0.001$) indicates significant difference compared to control cells. *** ($P < 0.001$) indicates significant difference compared to Pam3CSK4 treated cells. (d) HEK-Blue TM TLR3 cells were treated with PD180970 at a concentration range of 1 nM-10 μM in the presence of PIC (1 μg/ml) and assayed for SEAP activity for16 h. SEAP activity was quantified using HEK-Blue^{TM} Detection. PIC (1 μg/ml) was used as control for SEAP activity. PD180970 co-treated with PIC (1 μg/ml) caused no reduction in levels of NF-κB induced SEAP as compared to PIC alone. Data represents the group mean ± SEM; $n = 4$ per condition and experiments were repeated three times. $^{###}$ ($P < 0.001$) indicates significant difference compared to control cells. *** ($P < 0.001$) indicates significant difference compared to PIC treated cells. ns ($P > 0.05$) indicates no significant difference compared to PIC treated cells.

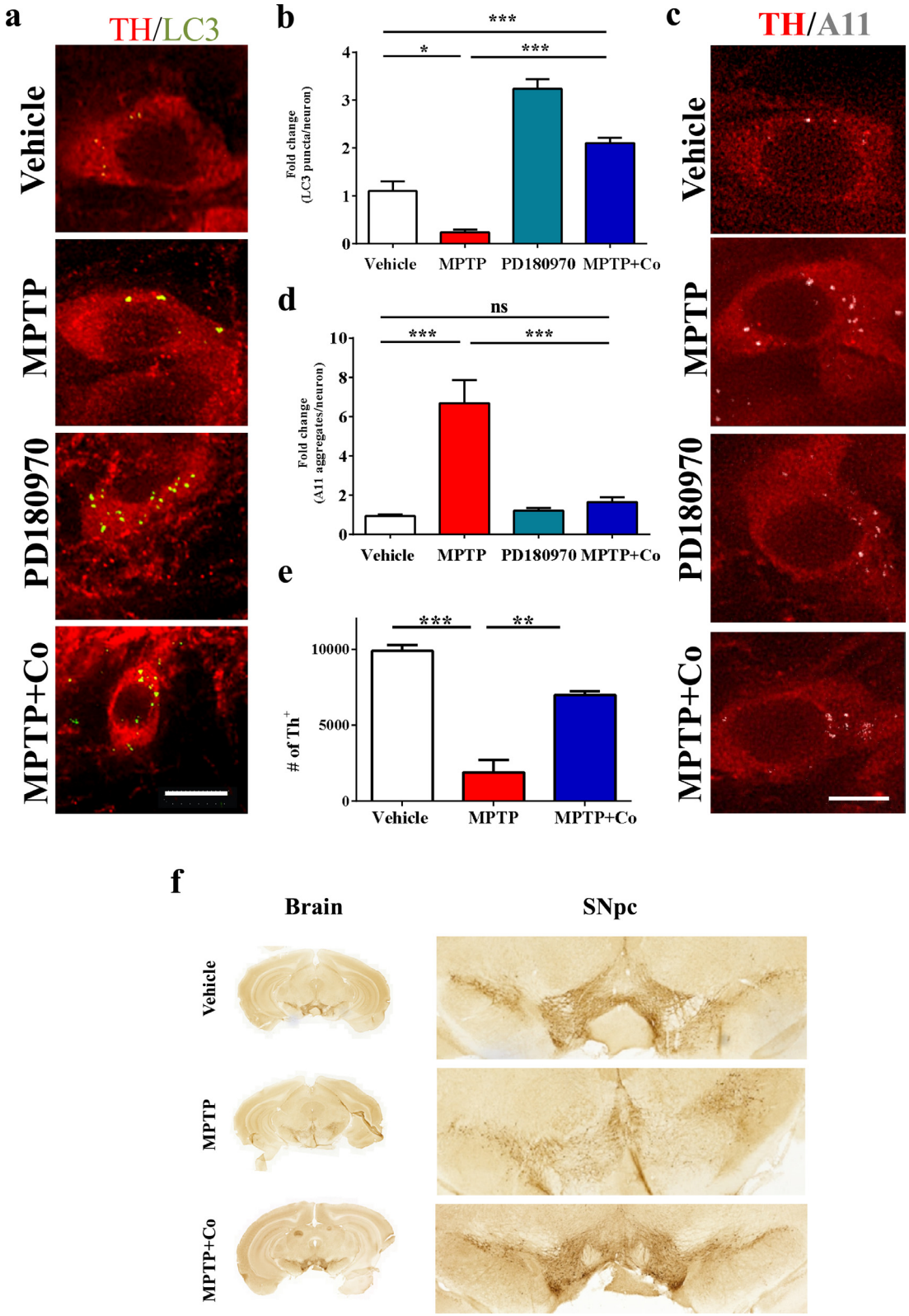

Fig. 5. PD180970 was neuroprotective by clearing toxic aggregates mediated through autophagy. (a and b) Fluorescent IHC microscopy images of DAergic neurons in SNpc that were dually stained for LC3 (the autophagy marker) and TH (the DAergic neuronal marker) proteins for various treatments such as vehicle, MPTP, PD180970 only and MPTP+Co ($n = 4$ animals per cohort) and LC3 puncta per neuron were quantitated. Scale bar was 70 μm. (c and d) Fluorescent IHC microscopy images of DAergic neurons in SNpc that were dually stained for A11 (the toxic protein oligomers marker) and TH proteins for all above mentioned treatments ($n = 4$ animals per cohort) and A11 puncta per neuron were quantitated. Scale bar was 50 μm. (e and f) Microscopy images of whole brain and SNpc for corresponding treatments such as vehicle, MPTP (23 mg/kg of body weight, 4 doses at 2 h intervals) and MPTP+Co (Co-administration of MPTP and PD: MPTP; 23 mg/kg of body weight and PD; 5 mg/kg of body weight, $n = 6$ animals per cohort). The unbiased stereological quantification of TH^+DAergic neurons in SNpc for above mentioned treatments were plotted. Statistical analysis was performed using one-way ANOVA and the post-hoc Bonferroni test. Error bars, mean ± SEM. ns-non-significant, *-$P < 0.05$, **-$P < 0.01$, ***-$P < 0.001$.

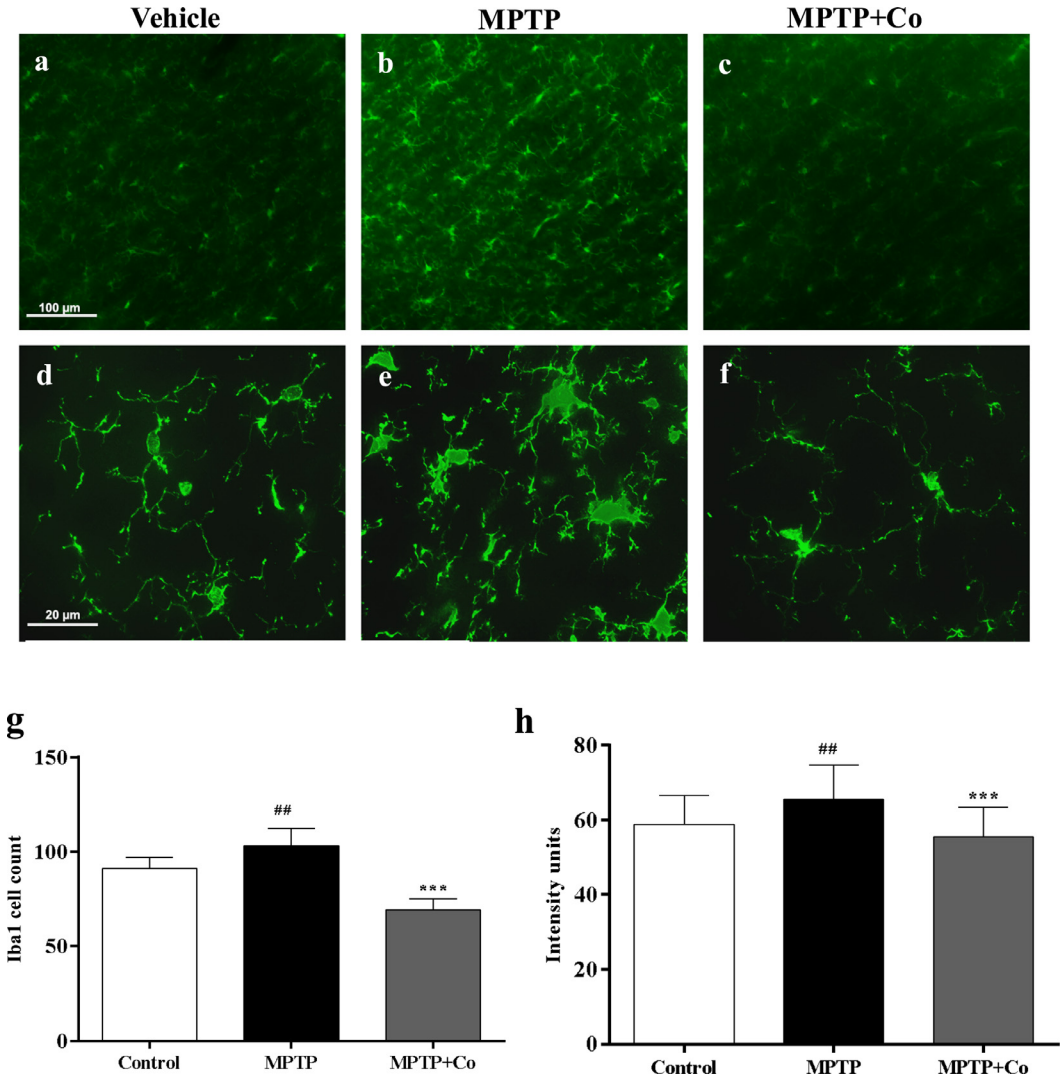

Fig. 6. PD180970 ameliorated microglial activation in vivo. (a–c) Low magnification images of mouse brain sections stained for Iba1. (d-f) High magnification images of mouse sections stained for Iba1. (g) Quantitative analysis of number of Iba1 expressing cells in mouse brain sections. PD180970 decreases number of activated microglia on activation by MPTP in mice brains. Mice were treated with MPTP or co-treated with PD180970 and MPTP (23 mg/kg bw in four doses on the treatment) for 7 days. Number of activated microglia was counted as Iba1 stained cells. PD180970 treatment showed significant reduction in number of activated microglia observed. Data represents the group mean ± SEM; $n = 3$ per condition; $^{\#\#}$ ($P < 0.01$) indicates significant difference compared to untreated mice (Control); **** ($P < 0.0001$) indicates significant difference compared to MPTP treated mice. (h) PD180970 decreases levels of activation marker Iba1 in microglia on activation by MPTP in mice brains. Mice were treated with MPTP or co-treated with PD180970 and MPTP (23 mg/kg bw in four doses on the treatment) for 7 days. Intensity of Iba1 staining was measured and PD180970 treatment showed significant reduction in intensity of Iba1 expression in activated microglia. Data represents the group mean ± SEM; $n = 3$ per condition; $^{\#\#}$ ($P < 0.01$) indicates significant difference compared to untreated mice (Control); *** ($P < 0.001$) indicates significant difference compared to MPTP treated mice.

turbed in MPTP-treated animals along with concomitant build-up of toxic protein oligomers. In PD180970 treated cohort, the LC3B puncta per neuron was up-regulated ($P < 0.001$, MPTP versus MPTP+PD180970, Fig. 5a and b) with significant decrease in toxic protein oligomers compared to MPTP treated cohort ($P < 0.001$, MPTP versus MPTP+PD180970, Fig. 5c and d). These results show that PD180970 treatment brought autophagy induction, which resulted in clearance of toxic protein oligomers in the DAergic neurons of SNpc.

15.9. PD180970 shows significant reduction in microglial activation when mice were treated with MPTP

Mice midbrain sections for Control, MPTP and MPTP+PD180970 treatments sections were stained for the microglial marker, Ionized calcium-binding adaptor molecule 1 (Iba1) [37]. Features of microglial activation, the Iba1 positive cell number and its intensity, were measured [38]. MPTP treatment significantly increased both the number of Iba1 positive cells and its intensity ($P < 0.01$, vehicle vs MPTP, Fig. 6a, b, d, e, g and h), thus confirming the MPTP-induced microglial proliferation and activation [20]. Upon PD180970 treatment, there was a significant downregulation in both the number of Iba1 positive cells and its intensity compared to the MPTP group ($P < 0.001$, MPTP vs MPTP+Co, Fig. 6b, c, e, f, g and h). These results indicate that PD180970 ablated the activation of microglia in vivo to exert the anti-neuroinflammatory effect.

15.10. PD180970 mitigates MPTP-induced behavioural impairments

Upon MPTP administration, these mice manifest Parkinsonian-like movement disorder such as exploratory and locomotory deficits. We used the rotarod (locomotory behaviour) and open field (exploratory behaviour) tests for assessing the ability of PD180970 to ameliorate the MPTP-induced behavioural deficits. The behavioural experiments were carried out on day 13 and day 15 of MPTP or saline administrations (Fig. S3).

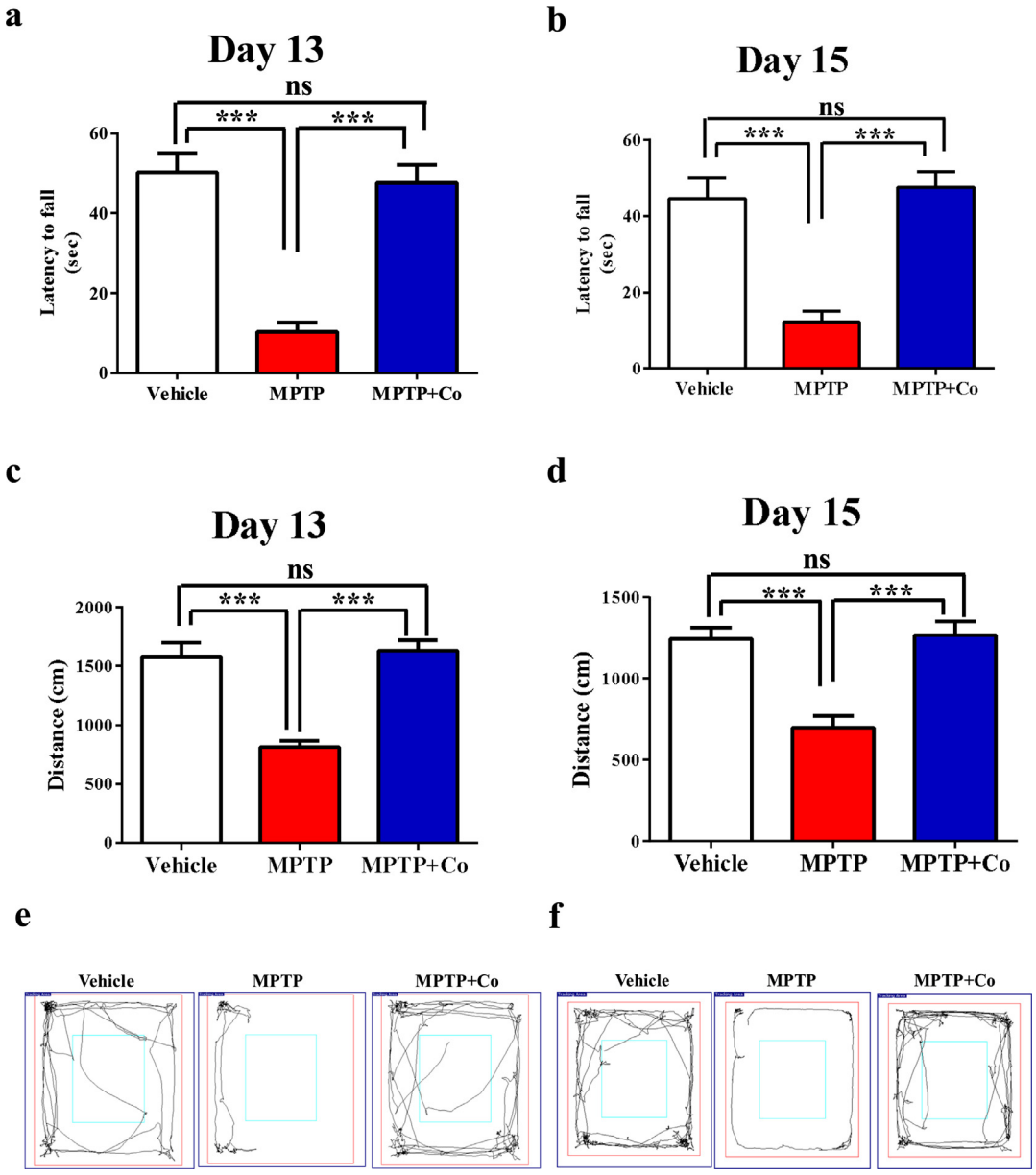

Fig. 7. PD180970 ameliorated the MPTP-mediated behavioral impairments. (a and b) Graphs indicating the calculated latency to fall (s) for various treatments such as vehicle, MPTP and MPTP+Co on both day 13 (a) and 15 (b) evaluated using rotarod test (n=at least 8 animals per group). Statistical analysis was performed using one-way ANOVA and the post-hoc Bonferroni test. Error bars, mean ± SEM. ns-non-significant, ***-$P < 0.001$. (c and d) Graphs indicating the peripheral distance travelled by mice across an open field arena evaluated using open field test on both day 13 (c) and 15 (d) (n=at least 8 animals per group). Statistical analysis was performed using one-way ANOVA and the post-hoc Bonferroni test. Error bars, mean ± SEM. ns-non-significant, ***-$P < 0.001$. (e and f) Representative trajectory path of mice travelled in an open field arena for all the mentioned groups on both day 13 (e) and day 15 (f).

In the rotarod test, latency to fall was significantly reduced in the MPTP cohort as compared to that of the saline cohort (day 13th and day 15th) ($P < 0.001$, vehicle versus MPTP, Fig. 7a and b), confirming its motor coordination impairments [6]. Interestingly, in PD180970 cohort, the latency to fall was significantly increased compared to MPTP cohort on both days ($P < 0.001$, MPTP versus MPTP+Co, Fig. 7a and b), and was found comparable to that of saline cohort on both days ($P > 0.5$, MPTP+Co versus saline, Fig. 7a and b).

The MPTP cohort also exhibited locomotory deficits, as it covered significantly lesser distance in open-field arena as compared to that of saline cohort on both day 13 and day 15 ($P < 0.001$, vehicle versus MPTP, Fig. 7c–f) [6]. The distance travelled by PD180970 cohort mice was significantly improved than that of MPTP cohort on both day 13 and day 15 ($P < 0.001$, MPTP versus MPTP+Co, Fig. 7c–f). Similar to our observation in rotarod test, the improvement in locomotory behaviour assessed through open field in PD180970 cohort mice was comparable to that of saline cohort on both days 13 and 15 ($P > 0.5$, MPTP+Co versus saline, Fig. 7c–f). To understand the consistency in the MPTP-induced motor impairments and also efficacy of small molecules, we performed the behaviour tests on both days 13 and 15. Thus, PD180970 treatment improved motor abilities to alleviate MPTP-induced behavioural impairments.

16. Discussion

In this study, we have concurrently identified and characterized the small molecule Bcr-Abl inhibitor, PD180970, as an aggrephagy and neuroinflammatory modulator in cultured mammalian cells and mouse models of Parkinson's disease. PD180970 induced-autophagy in mammalian cells and flux assays revealed that it

enhanced the formation of autophagosomes. PD180970, thus, protected neuronal cells against α-synuclein toxicity in an autophagy-dependent manner. In a preclinical mouse model of Parkinson's disease, we illustrated the neuroprotective ability of PD180970 in DAergic neurons of SNpc by clearing the toxic protein aggregates through enhancing autophagy. Interestingly, we noted that PD180970 ameliorates neuroinflammation through the TLR4-NF-κB axis mediated downregulation of proinflammatory cytokine release such as MCP-1 and IL-6 in vitro. This was further supported by results from mouse model of Parkinson's disease, where PD180970 treatment abrogated MPTP-induced microglial activation. This dual mechanism of PD180970 curbed neurodegeneration and resulted in the amelioration of MPTP-mediated motor behavioural deficits in the mice studies.

α-Synuclein protein aggregates are toxic to neuronal cells as they disrupt a plethora of cellular processes such as mRNA translation, endosome trafficking, redox balance, proteasome and autophagy [39]. The interplay of several factors make aggrephagy machinery dysfunctional during neurodegeneration pathogenesis that render neurons incompetent to cope with the increasing aggregate burden [5]. Thus, clearing toxic α-synuclein protein aggregates could be beneficial to enhance the neuronal viability and curb neurodegeneration related maladies [6]. The induction of autophagy either by genetic or pharmacological means has been shown to clear protein aggregates and alleviates neurodegeneration [6,7,40]. We show that PD180970 cytoprotects neuronal cells against α-synuclein-mediated toxicity in an autophagy-dependent manner. It induced autophagy by enhancing the autophagosomes in an mTOR-independent manner. Notably, we observed that PD180970 can induce autophagy in the dopaminergic neurons of the mice midbrain. mTOR independency of PD180970 is pharmacologically desirable as inhibiting mTOR inhibits important survival and growth-related pathways, leading to severe side effects such as immunosuppression and perturbed wound healing [5]. Recently treatment with another TKi, Nilotinib, prevented loss of dopaminergic neurons in lentiviral α-synuclein models through down-regulating caspase-3 activity [41].

Several studies in recent years have also suggested a potential role for TKi's in neurological disorders mediated through neuroinflammation, such as ischemic brain stroke, sub-arachnoid haemorrhage, Alzheimer's Disease and Multiple Sclerosis [42]. Imatinib, nilotinib and bosutinib have been shown to inhibit the production of pro-inflammatory cytokines (TNFα, IL-1β, IL-6) and thus attenuate recruitment of inflammatory cells to the central nervous system [41,43]. However, no such studies indicated the role of TKi's in neuroinflammation in Parkinson's disease models. A battery of in vitro studies including neuron-glia co-culture establishes the anti-neuroinflammatory potential of PD180970 by inhibiting the release of pro-inflammatory cytokines like MCP-1 and IL-6 (by greater than 6 and 3-fold respectively), the mediators of inflammation-induced neuronal cell death. Mechanistically, this anti-inflammatory activity is mediated through the TLR2 and TLR4 pathways by inhibiting NF-kβ and its downstream signalling pathway [44]. We validated the in vivo anti-neuroinflammatory role of PD180970 by demonstrating the subsiding microglial activation in SNpc region of midbrain. Recent studies have indicated that the common modes of microglial activation are the LPS/α-synuclein induced TLR4-NFκB pathway and the MPTP/Rotenone-induced ROS-NLRP3 inflammasome pathway, both of which work through tyrosine kinase c-Abl. PD180970, a c-Abl inhibitor could, thus, attenuate microglial activation through either axis. c-Abl activation has also been proposed to have an inhibitory effect on autolysosomes in microglia. A conserved mechanism in mDA neurons could also explain the increase in aggrephagy on PD treatment through inhibition of c-Abl [44,45].

Considering the unavailability of a cure for Parkinson's disease, a multi-pronged approach could potentially improve the chances of success of the therapy by increasing the different modes of action. Here, for the first time, our data present two crucial mechanisms through which this Bcr-Abl TKi, PD180970 can provide neuroprotection: 1) inducing neuronal autophagy, and 2) inhibiting microglia-mediated neuroinflammation.

In summary, the small molecule aggrephagy and neuroinflammatory modulator PD180970 may have therapeutic implications in neurodegenerative diseases such as Parkinson's disease and other synucleinopathies. This dual mode of action can be used as an early intervention drug in genetically predisposed individuals such as cases with prodromal Parkinson's disease as well therapeutically alongside dopamine supplementation for individuals in the latter phase of Parkinson's disease.

CRediT authorship contribution statement

Suresh SN: Conceptualization, Data curation. **Janhavi Pandurangi:** Data curation. **Ravi Murumalla:** Conceptualization. **Vidyadhara DJ:** Data curation. **Lakshmi Garimella:** Data curation. **Achyuth Acharya:** Data curation. **Shashank Rai:** Data curation. **Abhik Paul:** Data curation. **Haorei Yarreiphang:** Data curation. **Malini S Pillai:** Data curation. **Mridhula Giridharan:** Data curation. **James P Clement:** Funding acquisition, Methodology, Project administration, Resources, Software, Supervision. **Phalguni Anand Alladi:** Funding acquisition, Methodology, Project administration, Resources, Software, Supervision. **Taslimarif Saiyed:** Funding acquisition, Methodology, Project administration, Resources, Software, Supervision. **Ravi Manjithaya:** Funding acquisition, Methodology, Project administration, Resources, Software, Supervision, Writing - review & editing.

Acknowledgements

This work was supported by Wellcome Trust/DBT India Alliance Intermediate Fellowship (500159-Z-09-Z), DST-SERB grant (EMR/2015/001946), DBT (BT/INF/22/SP27679/2018) and JNCASR intramural funds to RM, and SERB, DST (SR/SO/HS/0121/2012) to PAA, and DST-SERB (SB/YS/LS-215/2013) to JPC and BIRAC funding to ETA C-CAMP. The funders have no role in study design, data collection, data analysis, interpretation, writing of the report. Application of PD180970 in autophagy modulation and neurodegeneration is patent pending.

Supplementary materials

Supplementary material associated with this article can be found, in the online version, at doi:10.1016/j.ebiom.2019.10.036.

References

[1] Wakabayashi K, Tanji K, Mori F, Takahashi H. The Lewy body in Parkinson's disease: molecules implicated in the formation and degradation of alpha-synuclein aggregates. Neuropathology 2007;27(5):494–506.
[2] Lykkebo S, Jensen PH. Alpha-synuclein and presynaptic function: implications for Parkinson's disease. Neuromolecular Med 2002;2(2):115–29.
[3] Luk KC, Kehm V, Carroll J, et al. Pathological alpha-synuclein transmission initiates Parkinson-like neurodegeneration in nontransgenic mice. Science 2012;338(6109):949–53.
[4] Cheng HC, Ulane CM, Burke RE. Clinical progression in Parkinson disease and the neurobiology of axons. Ann Neurol 2010;67(6):715–25.
[5] Suresh SN, Verma V, Sateesh S, Clement JP, Manjithaya R. Neurodegenerative diseases: model organisms, pathology and autophagy. J Genet 2018;97(3):679–701.
[6] Suresh SN, Chavalmane AK, Dj V, et al. A novel autophagy modulator 6-Bio ameliorates SNCA/alpha-synuclein toxicity. Autophagy 2017;13(7):1221–34.

[7] Suresh SN, Chavalmane AK, Pillai M, et al. Modulation of autophagy by a small molecule inverse agonist of ERRalpha is neuroprotective. Front Mol Neurosci 2018;11:109.
[8] Rajasekhar K, Suresh SN, Manjithaya R, Govindaraju T. Rationally designed peptidomimetic modulators of abeta toxicity in Alzheimer's disease. Sci Rep 2015;5:8139.
[9] Nixon RA. The role of autophagy in neurodegenerative disease. Nat Med 2013;19(8):983–97.
[10] Dikic I, Elazar Z. Mechanism and medical implications of mammalian autophagy. Nat Rev Mol Cell Biol 2018;19(6):349–64.
[11] Fujikake N, Shin M, Shimizu S. Association between autophagy and neurodegenerative diseases. Front Neurosci 2018;12:255.
[12] Hirsch EC, Hunot S. Neuroinflammation in parkinson's disease: a target for neuroprotection. Lancet Neurol 2009;8(4):382–97.
[13] Block ML, Hong JS. Microglia and inflammation-mediated neurodegeneration: multiple triggers with a common mechanism. Prog Neurobiol 2005;76(2):77–98.
[14] Phani S, Loike JD, Przedborski S. Neurodegeneration and inflammation in Parkinson's disease. Parkinsonism Relat Disord 2012;18(Suppl 1):S207–9.
[15] Stansley B, Post J, Hensley K. A comparative review of cell culture systems for the study of microglial biology in Alzheimer's disease. J Neuroinflamm 2012;9:115.
[16] Wu XF, Block ML, Zhang W, et al. The role of microglia in paraquat-induced dopaminergic neurotoxicity. Antioxid Redox Signal 2005;7(5–6):654–61.
[17] Wang T, Pei Z, Zhang W, et al. MPP+-induced COX-2 activation and subsequent dopaminergic neurodegeneration. FASEB J 2005;19(9):1134–6.
[18] Nakamura Y, Si QS, Kataoka K. Lipopolysaccharide-induced microglial activation in culture: temporal profiles of morphological change and release of cytokines and nitric oxide. Neurosci Res 1999;35(2):95–100.
[19] Choi YH, Park HY. Anti-inflammatory effects of spermidine in lipopolysaccharide-stimulated BV2 microglial cells. J Biomed Sci 2012;19:31.
[20] Machado V, Zoller T, Attaai A, Spittau B. Microglia-Mediated neuroinflammation and neurotrophic factor-induced protection in the MPTP mouse model of Parkinson's disease-lessons from transgenic mice. Int J Mol Sci 2016;17(2).
[21] Brahmachari S, Karuppagounder SS, Ge P, et al. c-Abl and Parkinson's disease: mechanisms and therapeutic potential. J Parkinsons Dis 2017;7(4):589–601.
[22] Abushouk AI, Negida A, Elshenawy RA, et al. C-Abl inhibition; a novel therapeutic target for Parkinson's disease. CNS Neurol Disord Drug Targets 2018;17(1):14–21.
[23] Fowler AJ, Hebron M, Missner AA, et al. Multikinase ABL/DDR/SRC inhibition produces optimal effects for tyrosine kinase inhibition in neurodegeneration. Drugs R D 2019;19(2):149–66.
[24] Cowan-Jacob SW, Fendrich G, Floersheimer A, et al. Structural biology contributions to the discovery of drugs to treat chronic myelogenous leukaemia. Acta Crystallogr Sect D Biol Crystallogr 2007;63(Pt 1):80–93.
[25] La Rosee P, Corbin AS, Stoffregen EP, Deininger MW, Druker BJ. Activity of the BCR-ABL kinase inhibitor PD180970 against clinically relevant BCR-ABL isoforms that cause resistance to imatinib mesylate (Gleevec, STI571). Cancer Res. 2002;62(24):7149–53.
[26] Kanthasamy AG, Kitazawa M, Yang Y, Anantharam V, Kanthasamy A. Environmental neurotoxin dieldrin induces apoptosis via caspase-3-dependent proteolytic activation of protein kinase C delta (PKCdelta): implications for neurodegeneration in Parkinson's disease. Mol Brain 2008;1:12.
[27] Kimura S, Noda T, Yoshimori T. Dissection of the autophagosome maturation process by a novel reporter protein, tandem fluorescent-tagged LC3. Autophagy 2007;3(5):452–60.
[28] Furlong RA, Narain Y, Rankin J, Wyttenbach A, Rubinsztein DC. Alpha-synuclein overexpression promotes aggregation of mutant huntingtin. Biochem J 2000;346(Pt 3):577–81.
[29] Jackson-Lewis V, Przedborski S. Protocol for the MPTP mouse model of Parkinson's disease. Nat Protoc 2007;2(1):141–51.
[30] Vidyadhara DJ, Yarreiphang H, Raju TR, Alladi PA. Admixing of MPTP-Resistant and susceptible mice strains augments nigrostriatal neuronal correlates to resist MPTP-Induced neurodegeneration. Mol Neurobiol 2017;54(8):6148–62.
[31] Fu Y, Yuan Y, Halliday G, Rusznak Z, Watson C, Paxinos G. A cytoarchitectonic and chemoarchitectonic analysis of the dopamine cell groups in the substantia nigra, ventral tegmental area, and retrorubral field in the mouse. Brain Struct Funct 2012;217(2):591–612.
[32] Vidyadhara DJ, Yarreiphang H, Abhilash PL, Raju TR, Alladi PA. Differential expression of calbindin in nigral dopaminergic neurons in two mice strains with differential susceptibility to 1-methyl-4-phenyl-1,2,3,6-tetrahydropyridine. J Chem Neuroanat 2016.
[33] Jyothi HJ, Vidyadhara DJ, Mahadevan A, et al. Aging causes morphological alterations in astrocytes and microglia in human substantia nigra pars compacta. Neurobiol Aging 2015;36(12):3321–33.
[34] Ikenoue T, Hong S, Inoki K. Monitoring mammalian target of rapamycin (mTOR) activity. Methods Enzymol 2009;452:165–80.
[35] Gabay C. Interleukin-6 and chronic inflammation. Arthritis Res Ther 2006;8 Suppl 2:S3.
[36] Sengupta U, Nilson AN, Kayed R. The role of amyloid-beta oligomers in toxicity, propagation, and immunotherapy. EBioMedicine 2016;6:42–9.
[37] Nakamura R, Nishimura T, Ochiai T, Nakada S, Nagatani M, Ogasawara H. Availability of a microglia and macrophage marker, iba-1, for differential diagnosis of spontaneous malignant reticuloses from astrocytomas in rats. J Toxicol Pathol 2013;26(1):55–60.
[38] Hoogland IC, Houbolt C, van Westerloo DJ, van Gool WA, van de Beek D. Systemic inflammation and microglial activation: systematic review of animal experiments. J Neuroinflammation 2015;12:114.
[39] Wong YC, Krainc D. alpha-synuclein toxicity in neurodegeneration: mechanism and therapeutic strategies. Nat Med 2017;23(2):1–13.
[40] Guo F, Liu X, Cai H, Le W. Autophagy in neurodegenerative diseases: pathogenesis and therapy. Brain Pathol 2018;28(1):3–13.
[41] Lonskaya I, Hebron ML, Selby ST, Turner RS, Moussa CE. Nilotinib and bosutinib modulate pre-plaque alterations of blood immune markers and neuro-inflammation in Alzheimer's disease models. Neuroscience 2015;304:316–27.
[42] Gagalo I, Rusiecka I, Kocic I. Tyrosine kinase inhibitor as a new therapy for ischemic stroke and other neurologic diseases: is there any hope for a better outcome. Curr Neuropharmacol 2015;13(6):836–44.
[43] Azizi G, Haidari MR, Khorramizadeh M, et al. Effects of imatinib mesylate in mouse models of multiple sclerosis and in vitro determinants. Iran J Allergy Asthma Immunol 2014;13(3):198–206.
[44] Lawana V, Singh N, Sarkar S, et al. Involvement of c-Abl kinase in microglial activation of NLRP3 inflammasome and impairment in autolysosomal system. J Neuroimmune Pharmacol 2017;12(4):624–60.
[45] Heneka MT, McManus RM, Latz E. Inflammasome signalling in brain function and neurodegenerative disease. Nat Rev Neurosci 2018;19(10):610–21.